치의과학석사 학위논문

Immune cells in tumor microenvironment control anti-cancer immunity in a rat oral carcinogenesis model

구강암 종양미세환경 면역세포의 항암면역작용 조절에 관한 연구

2023 년 2 월

서울대학교 대학원

치의과학과 구강악안면외과학 전공

최 용 석

Immune cells in tumor microenvironment control anti-cancer immunity in a rat oral carcinogenesis model

지도 교수 박 주 영

이 논문을 치의과학석사 학위논문으로 제출함
2023 년 2 월

서울대학교 대학원
치의과학과 구강악안면외과학 전공
최 용 석

최용석의 치의과학석사 학위논문을 인준함
2023 년 2 월

위 원 장 _____ 명 훈 _____ (인)

부위원장 _____ 박 주 영 _____ (인)

위 원 _____ 최 성 원 _____ (인)

Abstract

1. Introduction

A tumor microenvironment refers to an ecosystem that surrounds a tumor and includes host immune cells, extracellular matrix, blood vessels, and fibroblasts. These components of the tumor microenvironment (TME) exist around tumor cells and play a role in activating or inhibiting tumor growth. Therefore, understanding the role of each component in the TME became crucial in cancer research, especially the immune cells which are the key element for customized anti-cancer immunotherapy. Importantly, location and composition of immune cells differ among the cancer variants, and those in oral squamous cell carcinoma have not been extensively studied. Therefore, this study aims to elucidate the composition and role of immune cells in early precancerous lesions using a drug-induced oral squamous cell carcinoma model in rats. In addition, we would like to analyze the phenotypical and functional changes of the immune cells in the cervical lymph nodes (LNs) where the major immune reactions and cancer metastasis occur.

2. Materials and methods

The precancerous lesion in the oral mucosa was developed in 8-week-old Sprague Dawley (SD) female rats by 4-Nitroquinoline 1-oxide (4NQO) diluted drinking water for 8 weeks. Malignant changes were histologically analyzed by H&E and immunohistochemical staining (IHC) with p40, p63, and CK-HMW tumor markers. To analyze composition and the subtypes of immune cells in the TME, the oral mucosa was harvested from the sublocations such as tongue, buccal, and palatal

mucosa from the rats, and immune cells were isolated by using a combination of digestion enzymes. Neutrophils, T, B lymphocytes, macrophages, and dendritic cells were identified by flow cytometry using immune cell surface markers. Cervical LNs were collected, and frequency, number, phenotype, and cytokine secretion of the immune cells were analyzed by flow cytometry. The location of the immune cells in the oral mucosal TME and LNs was analyzed by IHC staining using anti-CD3, CD4, CD8, CD68, Bcl6, and PD-1 antibodies. The difference between the control and the experimental group was evaluated by statistical analysis using Mann-Whitney U test and p value of less than 0.05 was considered significant.

3. Results

H&E and IHC staining using tumor markers showed development of precancerous lesions in the oral mucosa of the rats in 4NQO drinking group. The frequency of $CD45^+$ total immune cells was significantly increased in oral precancerous lesions, and increased infiltration of $CD3^+$ T cells and $CD68^+$ macrophages was observed around the lamina propria. However, the number of immune cells in the oral mucosa TME of the 4NQO group was comparable to those of the control group. Interestingly, cervical LNs showed a significant increase in the size and number of immune cells in the 4NQO group. In particular, the number of $CD3^+$ T cells and the number of $CD8^+$ cytotoxic T cells were dramatically increased, confirming the increase in anti-cancer T cells in the draining LNs. Importantly, the expression of PD-1, an T cell exhaustion marker, and the frequency and number of $CD4^+CD25^+Foxp3^+$ regulatory T cells were significantly increased in the cervical LNs of the 4NQO group compared to the control group indicating suppressive

immune mechanism developed simultaneously. As a result, it was confirmed that the anti-cancer T cell immunity and the immune suppression coexist in the cervical LNs of the 4NQO induced rat cancer genesis model.

Keyword: oral squamous cell carcinoma, carcinogenesis, precancerous conditions, regulatory T cell, cytotoxic T cell, tumor microenvironment

Student Number: 2021-29761

Table of Contents

Introduction

Cancer of the oral cavity is one of the most common malignancies, especially in developing countries, but also in the developed world(Montero and Patel, 2015). Oral cavity cancer impacts on quality of life of patients, caused mainly by relatively low responsiveness to surgical, chemo, and radiological treatment, severe drug resistance, and post-treatment complications(Chuang et al., 2008; Min et al., 2017; Siegel et al., 2013; Vignali et al., 2008). Among the various oral cavity cancers, squamous cell carcinoma is the most common histology, and the oral squamous cell carcinoma (OSCC) develops at the various oral sublocations such as lip, tongue, floor of mouth, gingiva, buccal mucosa, retromolar trigone, hard palate, and oropharynx(Montero and Patel, 2015). The 5-year survival rate of the OSCC is 50% despite the advances in treatment modalities for solid tumors(Warnakulasuriya, 2009), establishing OSCC as the 7th and 9th cause of death worldwide for males and females, respectively(Znaor et al., 2013). Interestingly, the incidence of OSCC in woman and young individuals has been increasing in recent 10 years in South Korea, proposing that prevention and early diagnosis of the disease has become more important(Jeon et al., 2017; Lee et al., 2020). Furthermore, the overall survival rate of OSCC has not been changed(Bello et al., 2010; Choi et al., 2014; Kim et al., 2022; van Dijk et al., 2016), emphasizing that new diagnosis and treatment modalities should be developed which are specifically customized for OSCC.

Numerous studies have been conducted previously to promote early diagnosis and treatment for better prognosis of OSCC. The main etiological factors of OSCC are known as tobacco and alcohol use(Graham et al., 1977; Lee et al., 2020; Lingen et

al., 2008). However, the carcinogenesis of OSCC is considered a complex multistep process and have been studied extensively over the past decades focusing on the proliferation and uncontrolled growth of the tumor cells. Because normal oral mucosal keratinocytes are chronically exposed to risk factors, which can break the homeostasis and generate genetic instability. Key genetic alterations inside the normal epithelial cells occur in the genes such as TP53, NOTCH1 (Notch homolog 1, translocation-associated), EGFR (epidermal growth factor receptor), CDKN2A (cyclin-dependent kinase inhibitor 2a), STAT3 (signal transducer and activator of transcription 3), Cyclin D1, Rb (retinoblastoma), and LOH (loss of heterozygosity)(Curry et al., 2014; Tanaka and Ishigamori, 2011). Activation of proto-oncogenes such as ras, myc, and EGFR or inhibition of tumor suppressor genes such as TB53, pRb, and p16 by environmental factors; chemicals, irradiation, smoking, and viral infection are also known as main gene alterations in carcinogenesis of the epithelial cells(Tanaka and Ishigamori, 2011).

In recent years however, the outlook on cancer has changed dramatically and the tumor is no longer viewed as a bulk of malignant cancer cells, but rather as a complex TME(Giraldo et al., 2019). In TME, other subpopulations of cells interact with the cancer cells and get recruited to form a new ecosystem of the cells. The stromal component of TME is composed of multiple different cell types, such as cancer-associated fibroblast, neutrophil, macrophage (Mϕ), regulatory T cell (Treg), myeloid-derived suppressor cell (MDSC), natural killer cell (NK cell), platelets, and mast cells. These cellular subpopulations interact with each other as well as with cancer cells via complex communication networks through secretion of various cytokines, chemokines, growth factors, and proteins of the extracellular matrix(Altorki et al., 2019; Curry et al., 2014; Kalogirou et al., 2021; Rivera, 2015).

Based on the recent studies, understanding the role of each component of the TME became crucial in cancer research, especially the immune cells which are the key element for the customized anti-cancer immunotherapy. Importantly, location and composition of the TME immune cells differ among the cancer variants(Altorki et al., 2019; Curry et al., 2014), and those in OSCC have not been extensively studied. Importantly, several recent studies have shown that the oral mucosa has a unique composition of immune cells, such as higher frequency of $CD4^+$ T cells and Treg cells(Park et al., 2017; Park et al., 2018). Those studies utilized the modified protocol for the efficient isolation of the immune cells using combination of digestion enzymes and identified immune cell subsets in the rodent oral mucosa. Although the individual immune cell related markers such as CD44, CD105, and Bcl2 had been studied as a pro-cancer or anti-cancer markers for OSCC (Oliveira and Ribeiro-Silva, 2011), investigation of the overall immune cell subpopulations in OSCC TME using whole sets of immune cell surface markers can be one of the most crucial subjects in the oral cancer studies(Chao et al., 2021). Therefore, this study aims to elucidate the composition and role of immune cells in early precancerous lesions using a drug induced OSCC model in rats. In addition, we would like to analyze the phenotypical and functional changes of the immune cells in the cervical draining LNs where the major immune reactions and cancer metastasis occur.

Materials and methods

Animal

Female SD rats (body weight 130-140g) were purchased from Orient-Bio (Gapyeong, South Korea) and bred in the animal laboratory of Dental Research Institute in Seoul National University under the approval of Institutional Animal Care and Use Committee (SNU-210823-3-2). Animal experiments were performed with total 100 rats aged as 8- to 16-week-old.

Carcinogenesis of oral mucosa in rats

For induction of OSCC, 8-week-old rats were allowed to drink 50ppm of 4NQO diluted water for 8 weeks. The water bottle was replaced every one week, and the condition of rats was carefully monitored during the experiment by a veterinarian of the animal facility.

Dissection of oral mucosa sublocations

Three sublocations of rat oral mucosa (tongue, buccal cheek, and palate) were dissected after tissue perfusion using normal saline into the left ventricle of heart (Fig. 1). Superficial cervical draining LNs were obtained from both neck area and total 6 LNs were harvested. The harvested LNs were either processed for cell surface marker staining or fixed in 4% formalin for 24 hours, then embedded in paraffin for histological analysis.

Histological analysis using H&E and IHC staining

The paraffin embedded tissues were sectioned as 4μm thickness for histological

analysis. Tissue sections were deparaffinized with Neo-clear (Merck Millipore, USA) and rehydrated through different concentration of ethanol series (100%, 95%, 70%). The tissue slides were stained with H&E or stained with anti-CD3 (Abcam, clone SP7), anti-CD68 (Abcam, clone EPR23917-164), anti-CD4 (Abcam, clone CAL4), anti-CD8α (Abcam, clone CAL66), anti-BCL6 (Abcam, ab272859), anti-p63 (Abcam, clone EPR17863-47), anti-p40 (Abcam, clone EPR17863-47), CK-HMW (Thermo Fisher, clone KRTH 1076), and anti-PD-1 (Thermo Fisher, clone 7A11B1) for IHC. All slides were scanned using a slide scanner (Aperio CS2, Leica Biosystems, Nussloch, Germany) and the scanned images were captured using Aperio Imagescope (Leica Biosystems, Nussloch, Germany).

Isolation of immune cells from oral mucosa

The isolation procedures were followed by the previous studies(Park et al., 2017; Park et al., 2018). Liberase DL (Dispase low) and TL (Thermolysin low) were purchased from Roche, USA. After harvesting oral mucosal tissues according to the three sublocations, the tissues were chopped finely with a surgical scissor and incubated with Liberase DL (0.5 mg/ml) at 37°C for 20 minutes followed by Liberase TL (0.25 mg/ml) for another 20 minutes under mechanical rocking. Digestion enzyme reaction was stopped by addition of EDTA (1 mM), and digested tissues were filtered through a 70-μm cell strainer (BD Biosciences, USA). Collected cells were suspended with 40% Percoll solution (GE healthcare, USA), then centrifugated through a density gradient with 70% Percoll underneath (GE Healthcare, USA) for 25 min at 2,200 rpm with no brake. Leukocytes of cervical LNs were harvested between the 40% and the 70% Percoll solutions, then the harvested cells were washed 2 times and resuspended in immune cell culture media.

Flow Cytometry

The isolated immune cells were incubated with the fluorochrome conjugated anti-rat cell surface antibodies for 30 minutes at 4°C, then washed 2 times with flow cytometry wash buffer. The following antibodies were used for cell surface protein marker staining: CD8α (clone OX-8), IL-10 (clone A5-4), all from BD bioscience; CD161 (clone 3.2.3), CD11b/c (clone OX-42), CD45 (clone OX-1), CD3 (clone 1F4), TCRα/β (clone R73), TCRγ/δ (clone V65), CD4 (clone W3/25), Foxp3 (clone 150D), IL-4 (clone OX-81), all from Biolegend, USA; Granulocyte marker monoclonal antibody (clone HIS48), IFNγ (clone DB-1), TNFα (clone N3-19.1), IL-17A (clone Bio17B), B220 (clone HIS24), CD3 (clone UCHT1), CD25 (clone OX-39) all from Thermo fisher scientific, USA. Intracellular staining was performed with Foxp3/Transcription Factor Staining Buffer set (Thermfisher scientific, USA) according to the manufacturer's instruction. Before intracellular cytokine staining, the immune cells were stimulated *in vitro* with Phorbol 12-myristate 13-acetate (PMA) and Ionomycin for 4 hours at 37°C. The live immune cells were gated using forward scatter exclusion of dead cells stained with a Ghost Dye™ Viability Dyes (Tonbo, USA). Data was acquired on Cytoflex LX (Beckman, USA) and analyzed using FlowJo (BD, v10.8.1, USA).

Statistical analysis

GraphPad Prism 9 (GraphPad Software Inc., USA) was used for statistical analysis. Differences in flow cytometric results between control group and 4NQO group were evaluated with Mann-Whitney U test. Statistical significance was considered when $p < 0.05$.

Results

4NQO induced precancerous lesion in the rat oral mucosa

4NQO was administered to the rats at the dose of 50 ppm through drinking water to induce oral cancer in 8 weeks (Fig. 1A). After sacrifice, the sublocations of oral mucosa were dissected as shown in the Fig. 1B. The gross anatomy of the tongue in 4NQO drinking group showed rough and irregular surface accompanied with whitish and leukoplasia change compared to the tongue in control group (Fig. 2A). H&E staining of the tongue dorsal surface showed mild dysplasia of the epithelial cell layers such as increased cellular density, basal cell hyperplasia, hyperchromatic nuclei, bulbous drop shaped rete pegs, and hyper-keratinization (Fig 2B). However, degradation of the subepithelial basement membrane and local invasion into the underlying lamina propria were not observed, indicating precancerous lesion was induced by 4NQO administration. To confirm any malignant changes of the epithelial cells in the oral mucosa of the 4NQO group, IHC staining with tumor markers p63, p40 and CK-HMW was performed (Fig. 2B). The basal cell layer of the tongue dorsal surface of the 4NQO group showed more intense staining of p63, p40, and CK-HMW compared to the control group, strongly suggesting cancer genesis of the oral mucosa with DNA mutations at basal cell layer (Fig. 2B). Therefore, precancerous lesion with mild dysplasia of the oral mucosa was induced by 8 weeks administration of 4NQO in rats.

The total immune cells in the oral mucosa were increased and recruited to the lamina propria during carcinogenesis

To investigate the possible changes in frequency and number of the immune cells during carcinogenesis in the oral mucosa TME, the sublocations of oral mucosa was dissected and the isolated immune cells were analyzed by flow cytometry (Fig. 3A). The frequency of $CD45^+$ total immune cells were significantly increased in the oral mucosa of 4NQO group compared to control group, which means immunological reaction was active during the carcinogenesis (Fig. 3B and 3C). However, frequencies of other immune cells including $CD3^+$ T, NK, NKT, neutrophil and Mϕs were not changed in 4NQO group (Fig. 3C). Curiously, the numbers of $CD45^+$ total immune cells, $CD3^+$ T cells, and $CD3^-CD11b/c^+$ Mϕs were not different between control and 4NQO groups (Fig. 4A). Thus, we hypothesized that the absolute number of immune cells were not increased in oral mucosal TME but only recruited to the diseased site for the increased in frequency-wise, or they can actively circulate via lymphatic vessels to the draining LNs.

To test our hypothesis, we analyzed oral mucosa of two groups histologically using IHC staining with anti-rat anti-CD3 and CD68 antibodies. Surprisingly, $CD3^+$ cells and $CD68^+$ cells were increased and infiltrated in lamina propria of oral mucosa in 4NQO group, adjacent to the basement membrane of the oral epithelium. This recruitment was almost absent in the control group (Fig. 4B). In summary, our results suggested that the immune response during early carcinogenesis of the oral mucosa began with the recruitment of immune cells to the lamina propria and might circulate via draining LNs.

Anti-cancer immune response is driven by T cell in the draining cervical LN during oral carcinogenesis

Because LNs are a reservoir of T and B lymphocytes and the downstream drainage

sites of antigens from the adjacent tissues, upstream tissues and the draining LNs have a close relationship immunologically with each other. The downstream draining LNs of the oral cavity are cervical LNs and there are 6 superficial LNs in the rodent animal models. To better understand the immune response occurring in the oral mucosal TME of 4NQO group, the 6 cervical LNs of each rat were dissected and immune cells were isolated and analyzed. In 4NQO group, cervical LNs showed significantly increased size and well-developed T cell zone and outer B cell zone, which indicated activation and proliferation of antigen experienced T and B cells (Fig. 5A). To quantify these changes, we performed flow cytometry analysis for the LN immune cells. The number of $CD45^+$ total immune cells was significantly increased in 4NQO group and the $CD3^+CD4^+$ T and $CD3^+CD8^+$ T cells also showed significantly increase in precancerous lesion whereas other subpopulation of immune cells (NK, NKT, Mϕ, and neutrophil) was not changed (Fig. 5B-C). In addition, we performed IHC staining for with anti-CD4, CD8, and BCL6 antibodies to examine the activity of T lymphocytes histologically. $CD4^+$, $CD8^+$, and $BCL6^+$ were intensely stained in all 4NQO groups (Fig. 6). These results indicated that anti-cancer immune response in the oral mucosa can be driven by T cell mediated responses.

To find out patrolling APCs could deliver tumor antigen into the cervical LNs, $p63^+$ tumor marker was stained, and the $p63^+$ cells were shown increased in the medulla of the 4NQO draining LN compared to control (Fig. 7). Surprisingly, those $p63^+$ cells at the central medullary zone of draining LN were co-localized with $CD68^+$ cells. The overlapping at the LN medulla indicated that the tumor antigens were delivered by APCs such as Mϕs and signaled to T and B cells in draining LNs for anti-tumor immune reaction (Fig. 7).

Immune suppression by Treg cells and PD-1 expression co-exist in the cervical LNs of 4NQO group

To find out whether the increased T cells really show an increased cytotoxic response, we stimulated T cells *in vitro* and analyzed cytotoxic cytokine secretion. Frequency of IFNγ producing LN $CD4^+$ T cells was significantly increased in the 4NQO group compared to control group, indicating Th1 cell prone anti-cancer immune response is dominant in the oral mucosa. However, frequencies of IFNγ or TNFα producing cytotoxic $CD8^+$ T cells were comparable in 4NQO group cervical LNs compared to control (Fig. 8). Thus, we assumed if there was a possible mechanism of immune suppression to inhibit cytotoxic anti-cancer T cell activity in the cervical LNs.

Representative mechanisms of suppression against host immune response are immune suppression of regulatory T cells and immune evasion through T cell exhaustion by PD-1 expression. To verify whether these two mechanisms occur in the cervical LNs during oral carcinogenesis, flow cytometry analysis of $CD4^+CD25^+Foxp3^+$ Treg cells was done, and PD-1 expression was studied by IHC using anti-rat anti PD-1 antibody. The result showed dramatically increased frequency and number of Treg cells in the cervical LNs of 4NQO group, indicating presence of strong immunosuppressive activity developed at the same time (Fig. 9.). Besides, PD-1 expression was found in T cell zone of 4NQO group which was shown by staining of $CD3^+$ T cells. The expression area of PD-1 overlapped almost perfectly with the CD3 expression, which possibly indicated anti-tumor T cell activation and T cell exhaustion were established simultaneously at the early oral carcinogenesis stage (Fig. 10).

Discussion

The oral cavity is one of the most frequently exposed sites to foreign antigens as it constantly encounters food-borne, water-borne, and air-borne antigens and other environmental insults(Park et al., 2017; Park et al., 2018). The oral mucosa is a critical barrier tissue that harbors a series of distinct immune cell subsets. Immune surveillance in the oral mucosa is important for both local and systemic immunity because the oral cavity is a heavily utilized route of pathogen entry and also serves as site of pathogen propagation. Because oral cancer cells or precancerous cells develop as antigens to the host immune cells in the oral mucosa, understanding the immune cells in the TME of the oral cancerous lesion is crucial to understand oral cancer biology and develop anti-cancer therapy.

Nonetheless, composition and phenotype of the lymphocyte pool in the oral mucosa TME in the oral cancer model remained poorly characterized. Therefore, our study tried to build an animal model of OSCC which is the most common type of histology among the oral cancers. Based on the previous animal models for the oral carcinogenesis, we chose 4NQO drinking water model which was the most accessible and repeatable model for the upper digestive tract cancer(Chao et al., 2021; Ishida et al., 2017; Montero and Patel, 2015). Besides, we had to choose a rodent model for precise analysis of the immune cells because of the cell surface markers of the immune cells were largely available for mice or rats. After 8 weeks of 4NQO feeding in rats, our results showed that the oral mucosa of the tongue, buccal cheek, and palate transformed into precancerous lesion shown in H&E and IHC staining using tumor markers. We expected that the anti-tumor immune cells should be recruited in the TME of the precancerous lesion, and indeed, the frequency of

$CD45^+$ immune cells were significantly increased in oral precancerous lesions, and increased infiltration of $CD3^+$ T cells and $CD68^+$ Mϕs was observed around the lamina propria of the oral epithelium in 4NQO group. These results showed for the first time that the oral mucosa TME had immune cell recruitment around malignant transformed epithelial cells, and it is possible that the cancer cells can be attacked by the host immune cells, but at the same time the host immune cells can be exhausted and failed to remove the cancer cells.

Interestingly, the composition of the immune cells such as NK, NKT, Mϕs, dendritic cells, neutrophils, $CD8^+$ T, and $CD4^+$ T cell was comparable between control and 4NQO groups. Although the location of the $CD3^+$ T cells and $CD68^+$ Mϕs were found adjacent to the lamina propria of the oral epithelium, the frequencies of the subpopulation of such immune cells were not changed in 4NQO group. It can be possibly explained that the immune cells in the oral mucosa circulate or recruited robustly through the cervical LNs, so that the numbers of the immune cells cannot be changed when antigen develops but only focused or collected nearby the diseased site(Park et al., 2017; Park et al., 2018).

Therefore, we have also looked at the immune cells in the cervical lymph nodes, because the prognosis of the oral cancer is decided by the lymph node metastasis(Choi et al., 2006; Choi et al., 2014; Kim et al., 2022; Kim et al., 2005; Li et al., 2022). Interestingly, when tumor antigen developed *in vivo*, the patrolling dendritic cells, Mϕs in the local tissues could capture the tumor antigen expressing cells and processed the antigens on cell surfaces. Those professional antigen presenting cells (APCs) would travel and circulate into the draining LNs and contact adaptive immune cells such as T cells inducing anti-tumor

activation(Reticker-Flynn et al., 2022; Xie et al., 2022). Indeed, in the case of cervical LNs in our study, a significant increase in the size and number of immune cells was observed compared to the control group. CD68+ Mϕ were co-localized with p63 tumor marker positive cells, which indicated circulation of the patrolling immune cells into the draining LNs. In particular, the number of $CD3^+$ T cells was greatly increased in the cervical LNs. Among them, the number of $CD8^+$ cytotoxic T cells significantly increased, confirming the increase in anti-cancer T cells after the tumor antigen is recognized. Interestingly, the expression of PD-1, a T cell exhaustion marker, was increased in T cells of the cervical LNs of the 4NQO group compared to control group. As a result, it was confirmed that the mechanism of suppressing the function of anti-cancer T cells occurred simultaneously in the cervical LNs of the oral carcinogenesis model.

Based on the results of this study, the immune cells in the TME of the oral precancerous lesion was investigated and their function of controlling anti-cancer immune reaction was studied. The immune cells in the draining LNs were also analyzed because the immune cells in the oral mucosa circulate via cervical LNs but the cancer cells metastasize through the LNs from the oral mucosa as well. Therefore, this study revealed one more time that the cervical LNs were the important location for the controlling oral cancer, because development of cytotoxic anti-cancer T cells, immune suppressive Treg cells, and T cell exhaustion occur simultaneously at the cervical LNs. From the understanding of the TME immune cells and their controlling function of oral carcinogenesis in this study, a new target for oral cancer immunotherapy can be identified in the further studies.

Figure 1. Establishment of the experimental precancerous lesions by administration of 4NQO and immune cell analysis in TME. A. Schematic diagram of the experimental procedures. B. The location of harvested oral mucosa.

A

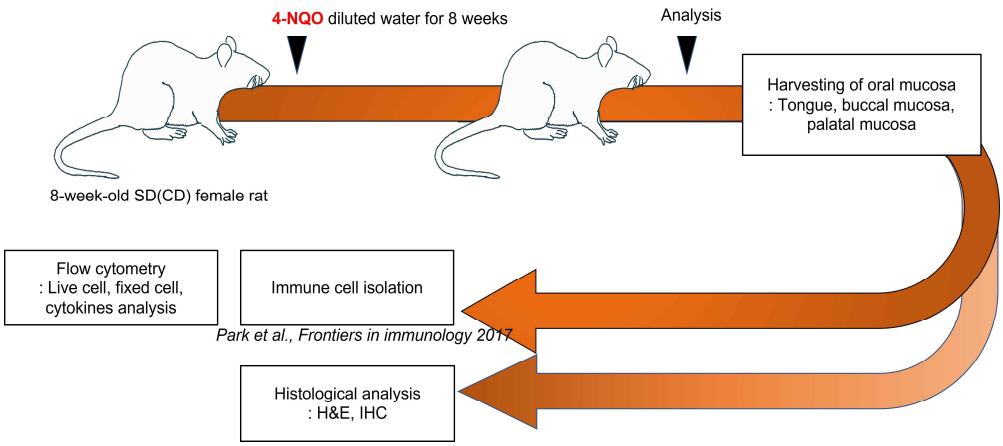

B

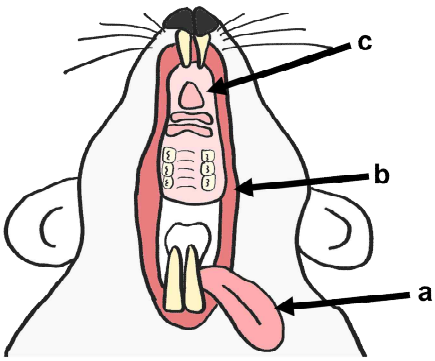

a. Tongue
b. Buccal mucosa
c. Palatal mucosa

Figure 2. **Histological analysis of tongue in control and 4NQO groups.** A. Gross anatomy of the dorsal surface of the tongue harvested from control and 4NQO groups. B. Increased epithelial dysplasia with basal cell hyperplasia, higher cell density, elongated rete ridges, and hyperchromatic nuclei were observed in H&E staining of tongue of 4NQO group. IHC staining using epithelial cancer markers p63, p40, and CK-HMW showed malignant change of the epithelial cells in 4NQO group. The lower magnification was shown in x 40 (left 2 columns) and the higher magnification was shown in x 200 (right 2 columns).

A

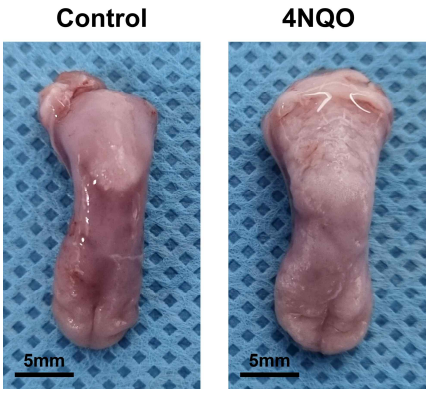

B

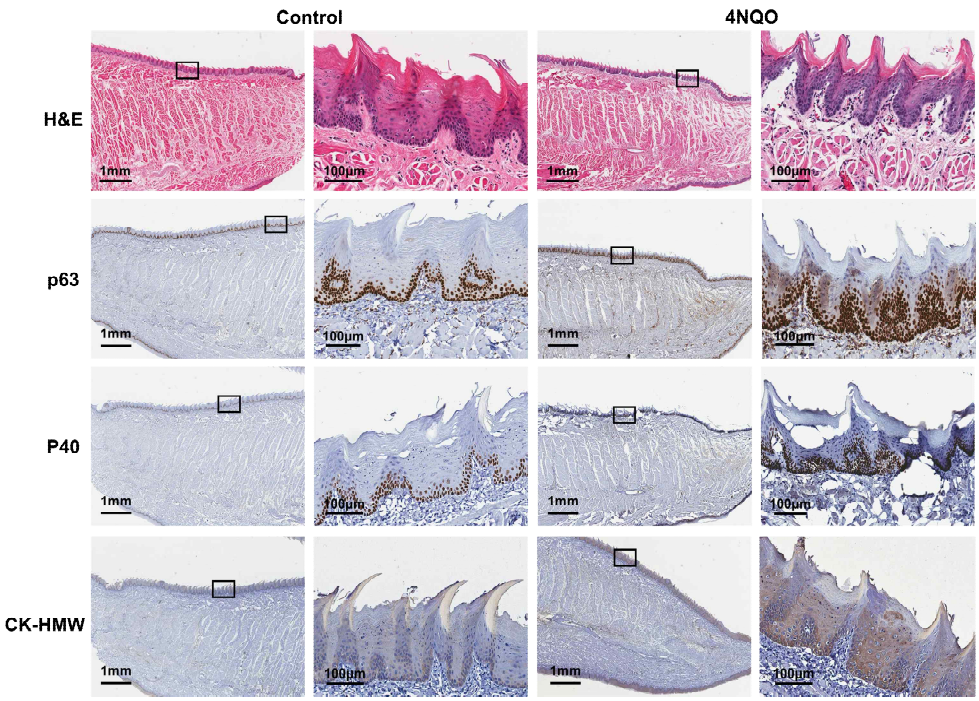

Figure 3. Analysis of immune cell subpopulations of oral mucosa TME by flow cytometry. A. Schematic diagram of immune cell isolation procedures from the rat oral mucosal tissues. B. Histogram and dot plot by flow cytometry show the frequencies of $CD3^+$ T cells and $CD11b/c^+CD3^-$ Mϕ in oral mucosal TME. C. Flow cytometry analysis showed the frequencies of various immune cell subpopulations in oral mucosal TME which was identified cell surface marker staining. 7 independent experiments were done with total 100 rats. Differences between control and 4NQO group were evaluated with Mann-Whitney U test. Statistical significance * was considered when $p < 0.05$.

A

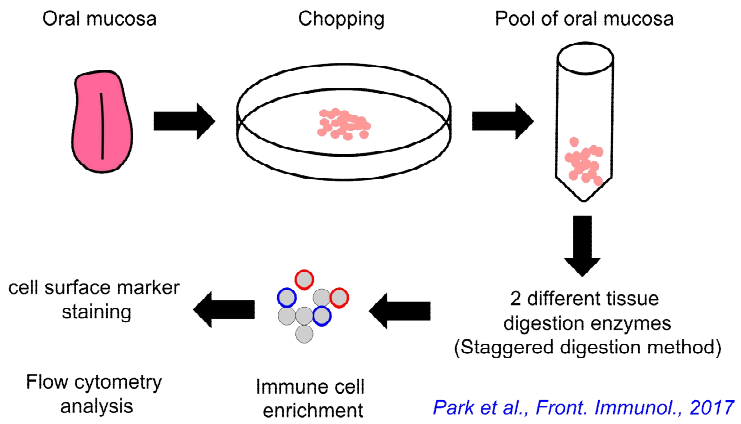

B

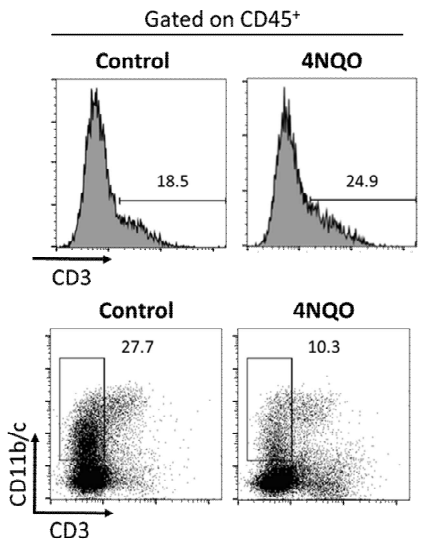

C

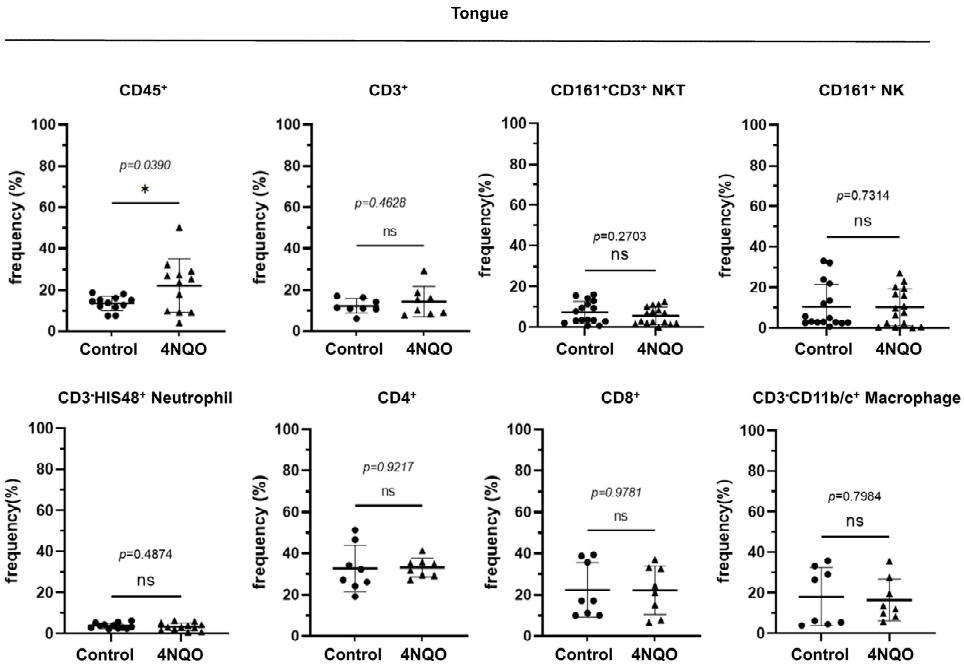
Tongue
CD45+
CD3+
CD161+CD3+ NKT
CD161+ NK
CD3-HIS48+ Neutrophil
CD4+
CD8+
CD3-CD11b/c+ Macrophage
frequency (%)
p=0.0390
*
p=0.4628
ns
p=0.2703
ns
p=0.7314
ns
p=0.4874
ns
p=0.9217
ns
p=0.9781
ns
p=0.7984
ns
Control
4NQO

Figure 4. Analysis of cell number and location of the immune cell subpopulations in oral mucosal TME. A. The numbers of $CD45^+$ total immune cells, $CD3^+$ T cells and $CD11b/c^+CD3^-$ Mϕs were comparable between control and 4NQO groups shown by flow cytometry. B. IHC staining showed increased numbers of $CD3^+$ T cell and $CD68^+$ Mϕs at the lamina propria adjacent to the basement membrane of the 4NQO group (red arrows). The lower magnification was shown in x 40 (left column) and the higher magnification was shown in x 200 (right column).

A

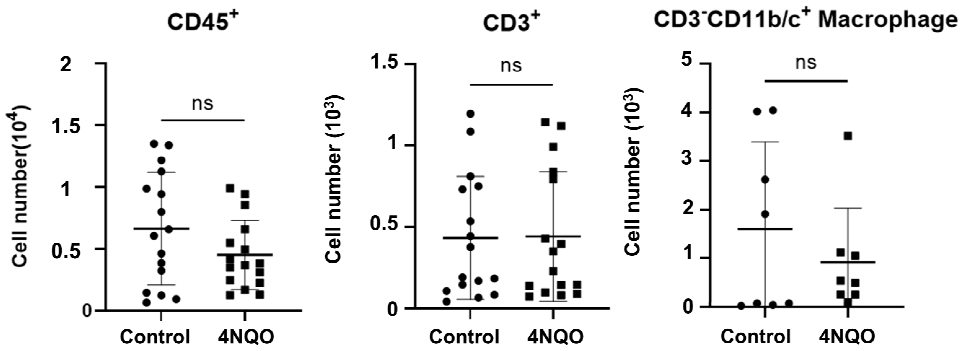

B

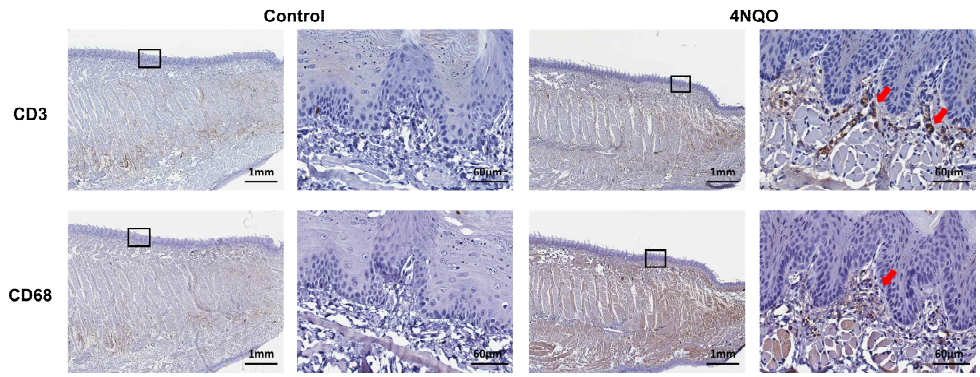

Figure 5. Analysis of cell number and location of the immune cell subpopulations in the draining cervical LNs. A. Cervical LNs of 4NQO group showed dramatically increased size and altered intranodal anatomical structures. Formation of the secondary B cell follicle (white arrow) and proliferation of T cell zone was clearly shown. The lower magnification was shown in x 20 (upper row) and the higher magnification was shown in x 200 (bottom row).

B. Cervical LNs of 4NQO group showed increased number of $CD45^+$ total immune cells, $CD3^+$ T, $CD4^+$ T, and $CD8^+$ T cells. C. The numbers of NK cells, NKT cells, Mϕ, neutrophils, and B cells were comparable between control and 4NQO groups. Differences between the groups were calculated with Mann-Whitney U test. Statistical significance *** was considered when p <0.001.

A

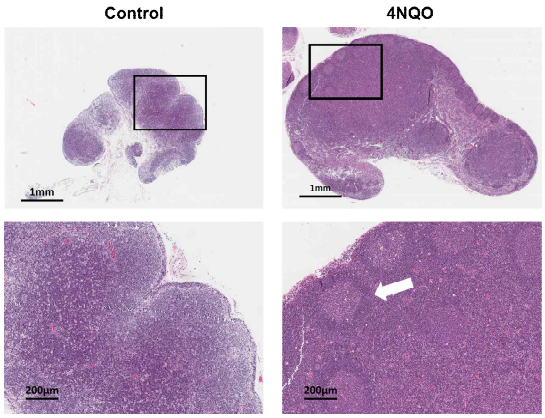

B

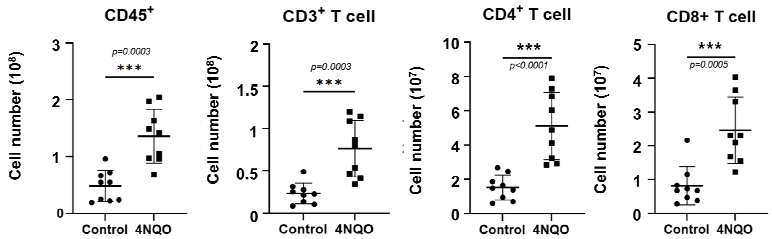

C

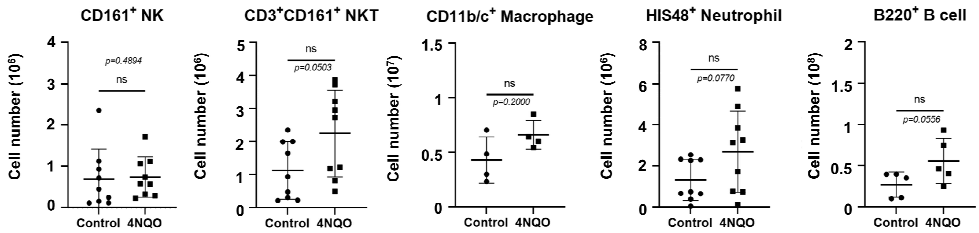

Figure 6. IHC staining of draining cervical LNs of 4NQO group showed proliferation of B and T cell zones and altered intranodal anatomy of LNs. $CD4^+$ and $CD8^+$ immune cells were located at the T and B cell zone of the cervical LN of 4NQO group. Anti-rat BCL6 antibody staining identified formation of the secondary follicles in the 4NQO group, indicating activation of T and B cell immune reactions. Magnification was shown in x 20 and the scale bars are 1mm.

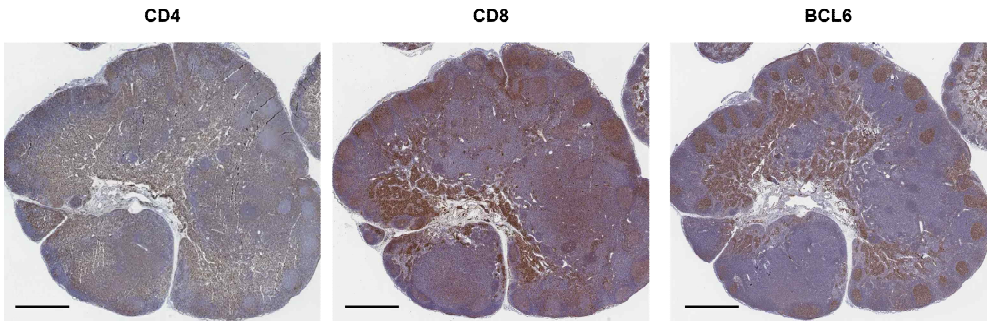

Figure 7. IHC staining of draining cervical LNs showed co-localization of Mϕs and cancer cells in the cervical LNs. CD68^{+} Mϕs and p63^{+} cancer cells were stained by IHC and clearly shown in the LNs of 4NQO group (right). CD68^{+} Mϕs and p63^{+} cancer cells were co-localized at the medulla of the LNs. Magnification was shown in x 20 and the scale bars are 1mm.

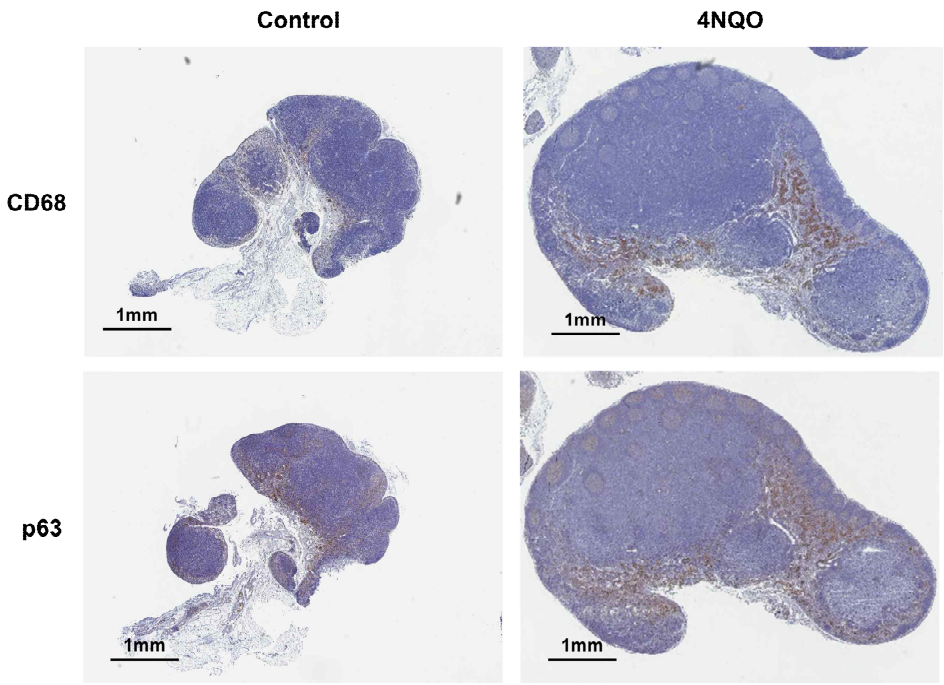

Figure 8. Analysis of cytokine expression of T cells in cervical LNs using flow cytometry. The LNs immune cells were isolated and stimulated *in vitro* with PMA and Ionomycin for cytokine expression staining. Frequency of IFNγ producing $CD4^+$ T cells was significantly increased in cervical LNs of 4NQO group. Differences between the groups were calculated with Mann-Whitney U test. Statistical significance ** was considered when p <0.01.

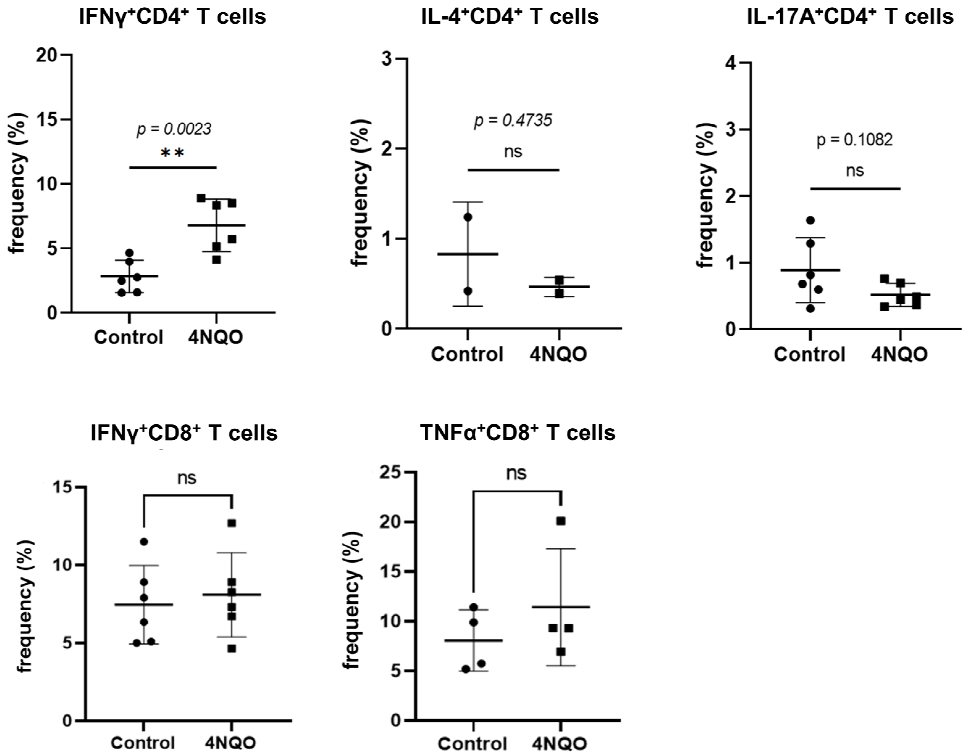

Figure 9. Increased Treg cells in the cervical LNs of 4NQO group. The frequency and the number of $CD4^{+}CD25^{+}Foxp3^{+}$ Treg cells were significantly increased in the cervical LNs of 4NQO group. Differences between the groups were calculated with Mann-Whitney U test. Statistical significance **** was considered when p <0.0001.

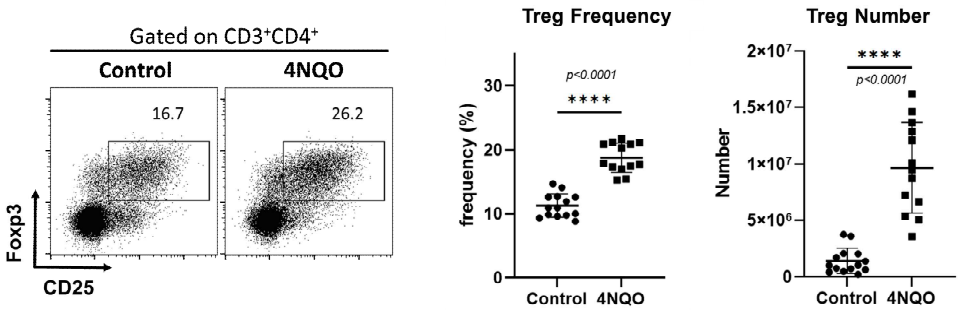

Figure 10. PD-1 is highly expressed in the cervical LNs of 4NQO group and the expression is co-localized with LN T cells. A. PD-1 is highly expressed in the T cell zone in the cervical LN of 4NQO group (red arrows). The lower magnification was shown in x 20 (left) and the higher magnification was shown in x 400 (right). Scale bars are 1mm. B. The expression of PD-1 (dotted line, left) in the cervical LN of 4NQO group was co-localized with $CD3^{+}$ T cells (dotted line, right). Magnification was shown in x 20 and the scale bars are 1mm.

A

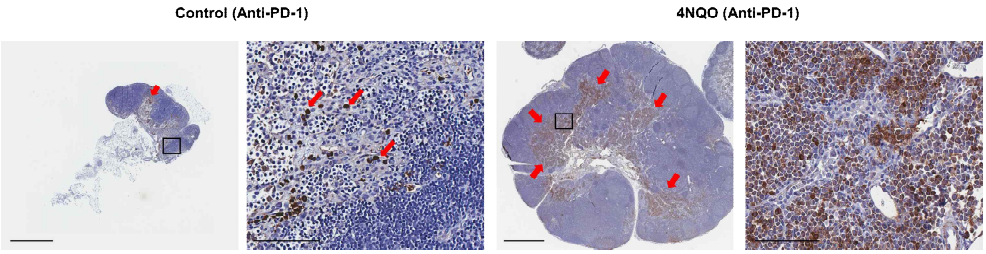

B

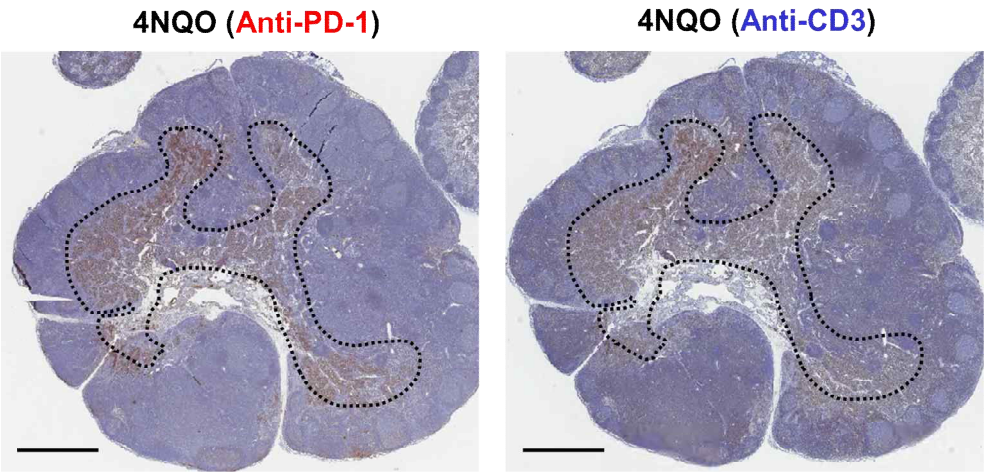

References

1. Altorki, N.K., Markowitz, G.J., Gao, D., Port, J.L., Saxena, A., Stiles, B., McGraw, T., and Mittal, V. (2019). The lung microenvironment: an important regulator of tumour growth and metastasis. Nat Rev Cancer *19*, 9-31.
2. Bello, I.O., Soini, Y., and Salo, T. (2010). Prognostic evaluation of oral tongue cancer: means, markers and perspectives (II). Oral Oncol *46*, 636-643.
3. Chao, J.L., Korzinkin, M., Zhavoronkov, A., Ozerov, I.V., Walker, M.T., Higgins, K., Lingen, M.W., Izumchenko, E., and Savage, P.A. (2021). Effector T cell responses unleashed by regulatory T cell ablation exacerbate oral squamous cell carcinoma. Cell Rep Med *2*, 100399.
4. Choi, K.K., Kim, M.J., Yun, P.Y., Lee, J.H., Moon, H.S., Lee, T.R., and Myoung, H. (2006). Independent prognostic factors of 861 cases of oral squamous cell carcinoma in Korean adults. Oral Oncol *42*, 208-217.
5. Choi, S.W., Moon, E.K., Park, J.Y., Jung, K.W., Oh, C.M., Kong, H.J., and Won, Y.J. (2014). Trends in the incidence of and survival rates for oral cavity cancer in the Korean population. Oral Dis *20*, 773-779.
6. Chuang, S.C., Scelo, G., Tonita, J.M., Tamaro, S., Jonasson, J.G., Kliewer, E.V., Hemminki, K., Weiderpass, E., Pukkala, E., Tracey, E. et al. (2008). Risk of second primary cancer among patients with head and neck cancers: A pooled analysis of 13 cancer registries. Int J Cancer *123*, 2390-2396.
7. Curry, J.M., Sprandio, J., Cognetti, D., Luginbuhl, A., Bar-ad, V., Pribitkin, E., and Tuluc, M. (2014). Tumor microenvironment in head and neck squamous cell carcinoma. Semin Oncol *41*, 217-234.
8. Giraldo, N.A., Sanchez-Salas, R., Peske, J.D., Vano, Y., Becht, E., Petitprez, F., Validire, P., Ingels, A., Cathelineau, X., Fridman, W.H. et al. (2019). The clinical role of the TME in solid cancer. Br J Cancer *120*, 45-53.
9. Graham, S., Dayal, H., Rohrer, T., Swanson, M., Sultz, H., Shedd, D., and Fischman, S. (1977). Dentition, diet, tobacco, and alcohol in the epidemiology of oral cancer. J Natl Cancer Inst *59*, 1611-1618.
10. Ishida, K., Tomita, H., Nakashima, T., Hirata, A., Tanaka, T., Shibata, T.,

and Hara, A. (2017). Current mouse models of oral squamous cell carcinoma: Genetic and chemically induced models. Oral Oncol *73*, 16-20.

11. Jeon, J.H., Kim, M.G., Park, J.Y., Lee, J.H., Kim, M.J., Myoung, H., and Choi, S.W. (2017). Analysis of the outcome of young age tongue squamous cell carcinoma. Maxillofac Plast Reconstr Surg *39*, 41.
12. Kalogirou, E.M., Tosios, K.I., and Christopoulos, P.F. (2021). The Role of Macrophages in Oral Squamous Cell Carcinoma. Front Oncol *11*, 611115.
13. Kim, M.G., Choi, Y.S., Youn, S.M., Ko, J.H., Oh, H.J., Lee, J.H., Park, J.Y., and Choi, S.W. (2022). Treatment outcomes and prognostic factors in oral tongue cancer: a 20-year retrospective study at the National Cancer Center, South Korea. J Korean Assoc Oral Maxillofac Surg *48*, 192-200.
14. Kim, M.J., Lim, K.Y., Kim, J.W., Nam, I.W., Lee, J.H., and Myoung, H. (2005). Stage and mRNA expression of survivin in lymph node as prognostic indicators in patients with oral squamous cell carcinoma. Cancer Lett *224*, 253-261.
15. Lee, S.U., Moon, S.H., Choi, S.W., Cho, K.H., Park, J.Y., Jung, Y.S., Ryu, J., Ryu, C.H., Yun, T., Kim, T.H. et al. (2020). Prognostic significance of smoking and alcohol history in young age oral cavity cancer. Oral Dis *26*, 1440-1448.
16. Li, T., Liu, T., Zhao, Z., Xu, X., Zhan, S., Zhou, S., Jiang, N., Zhu, W., Sun, R., Wei, F. et al. (2022). The Lymph Node Microenvironment May Invigorate Cancer Cells With Enhanced Metastatic Capacities. Front Oncol *12*, 816506.
17. Lingen, M.W., Kalmar, J.R., Karrison, T., and Speight, P.M. (2008). Critical evaluation of diagnostic aids for the detection of oral cancer. Oral Oncol *44*, 10-22.
18. Min, S.K., Choi, S.W., Ha, J., Park, J.Y., Won, Y.J., and Jung, K.W. (2017). Conditional relative survival of oral cavity cancer: Based on Korean Central Cancer Registry. Oral Oncol *72*, 73-79.
19. Montero, P.H., and Patel, S.G. (2015). Cancer of the oral cavity. Surg Oncol Clin N Am *24*, 491-508.
20. Oliveira, L.R., and Ribeiro-Silva, A. (2011). Prognostic significance of immunohistochemical biomarkers in oral squamous cell carcinoma. Int J

Oral Maxillofac Surg *40*, 298-307.

21. Park, J.Y., Chung, H., Choi, Y., and Park, J.H. (2017). Phenotype and Tissue Residency of Lymphocytes in the Murine Oral Mucosa. Front Immunol *8*, 250.
22. Park, J.Y., Chung, H., DiPalma, D.T., Tai, X., and Park, J.H. (2018). Immune quiescence in the oral mucosa is maintained by a uniquely large population of highly activated Foxp3(+) regulatory T cells. Mucosal Immunol *11*, 1092-1102.
23. Reticker-Flynn, N.E., Zhang, W., Belk, J.A., Basto, P.A., Escalante, N.K., Pilarowski, G.O.W., Bejnood, A., Martins, M.M., Kenkel, J.A., Linde, I.L. et al. (2022). Lymph node colonization induces tumor-immune tolerance to promote distant metastasis. Cell *185*, 1924-1942 e1923.
24. Rivera, C. (2015). Essentials of oral cancer. Int J Clin Exp Pathol *8*, 11884-11894.
25. Siegel, R., Naishadham, D., and Jemal, A. (2013). Cancer statistics, 2013. CA Cancer J Clin *63*, 11-30.
26. Tanaka, T., and Ishigamori, R. (2011). Understanding carcinogenesis for fighting oral cancer. J Oncol *2011*, 603740.
27. van Dijk, B.A., Brands, M.T., Geurts, S.M., Merkx, M.A., and Roodenburg, J.L. (2016). Trends in oral cavity cancer incidence, mortality, survival and treatment in the Netherlands. Int J Cancer *139*, 574-583.
28. Vignali, D.A., Collison, L.W., and Workman, C.J. (2008). How regulatory T cells work. Nat Rev Immunol *8*, 523-532.
29. Warnakulasuriya, S. (2009). Global epidemiology of oral and oropharyngeal cancer. Oral Oncol *45*, 309-316.
30. Xie, W., Shen, J., Wang, D., Guo, J., Li, Q., Wen, S., Dai, W., Wen, L., Lu, H., Fang, J. et al. (2022). Dynamic changes of exhaustion features in T cells during oral carcinogenesis. Cell Prolif *55*, e13207.
31. Znaor, A., van den Hurk, C., Primic-Zakelj, M., Agius, D., Coza, D., Demetriou, A., Dimitrova, N., Eser, S., Karakilinc, H., Zivkovic, S. et al. (2013). Cancer incidence and mortality patterns in South Eastern Europe in the last decade: gaps persist compared with the rest of Europe. Eur J Cancer *49*, 1683-1691.

국문초록

구강암 종양미세환경 면역세포의 항암면역작용 조절에 관한 연구

성 명 최용석
학과 및 전공 치의과학과 구강악안면외과학

1. 목 적

종양 미세환경이란 종양의 주위를 둘러싸는 숙주의 면역 세포, 세포외 기질, 혈관 및 섬유아세포를 포함하는 생태계를 의미한다. 이러한 종양 미세환경의 구성 요소들은 종양 세포의 주위에 존재하며 종양의 성장을 활성화하거나 억제하는 역할을 한다. 따라서 암 연구, 특히 맞춤형 항암치료를 개발하는 데 있어 종양 미세환경을 이해하는 것이 중요하며, 그중에서도 면역 세포의 구성과 그 위치는 암종마다 차이가 있어 항암연구 분야의 핵심이라 할 수 있다. 그러나 현재까지 구강 편평상피세포암 및 구강 전암병소의 종양 미세환경 면역 세포의 구성과 위치, 역할에 관한 연구는 부족한 실정이다. 따라서 본 연구에서는 약물로 유도된 구강 편평상피세포암 동물 구강 점막 모델을 이용하여 초기 전암 병소의 면역 세포 구성과 그 역할을 밝히고자 한다. 또한, 구강암의 전이가 일어나는 경부 임파절에서 전암병소 발생 시에 나타나는 면역 세포의 변화와 항암면역 세포가 암세포 전이를 조절하는 기전에 관해 연구하고자 한다.

2. 방 법

8주령의 SD 암컷 백서에 발암물질인 4NQO(4-Nitroquinoline 1-oxide)가 희석된 식수를 8주간 섭취시켜 구강 점막에 초기 전암 병소의 발생을 유도하였다. 구강 점막의 암화를 확인하기 위해 H&E 염색 및 p40, p63, CK-HMW 종양 마커의 면역조직화학 염색을 시행하였다. 종양 미세환경 면역 세포의 구성을 분석하기 위하여 구강 점막을 혀, 볼, 구개 점막으로 구분하여 채취하여 기존 발표된 프로토콜에 따라 면역 세포를 분리하고 유세포분석을 통하여 T, B 임파구, 대식세포, 수지상세포, 중성구 등의 면역 세포 구성을 분석하였다. 6개의 경부 임파절을 채취하여 유세포 분석을 통한 면역 세포 구성 및 사이토카인 분비 기능을 분석하였다. 병소 및 경부 임파절에서 면역 세포의 위치와 기능은 CD3, CD4, CD8, CD68, Bcl6, PD-1 등의 면역 세포 마커 염색을 통한 면역조직화학 염색을 시행하였다. 대조군과 실험군의 차이에 대해 Mann-Whitney test를 이용하여 p-값을 계산하였으며, $p < 0.05$인 경우를 통계학적으로 유의성으로 정의하였다.

3. 결 과

H&E 염색 및 종양 마커를 이용한 면역조직화학 염색상 4NQO를 섭취한 백서의 구강 점막에서 전암병소의 발생이 관찰되었다. 구강 전암병소 내에는 $CD45^+$ 면역 세포의 빈도가 유의하게 증가하였으며, $CD3^+$ T 세포 및 $CD68^+$ 대식세포의 침윤 증가가 lamina propria 주위에서 관

찰되었다. 그러나 구강점막의 종양미세환경 내 면역세포의 숫자에는 실험군과 대조군 사이에 유의한 차이가 없었다. 반면에 경부 임파절의 경우, 실험군에서 임파절의 크기와 임파절 내 면역세포 수의 유의한 증가 양상이 관찰되었으며, 특히 $CD3^+$ T 세포의 수가 매우 증가하였는데, 이 중 $CD8^+$ 세포독성 T 세포의 숫자가 증가하여 항암 T 세포의 증가를 확인할 수 있었다. 흥미롭게도 4NQO 백서의 경부 임파절의 T 세포에서 피로 마커인 PD-1의 발현이 대조군에 비해 유의하게 증가된 양상이 관찰되었으며 이와 동시에 숙주의 면역 기능을 억제하는 $CD4^+CD25^+Foxp3^+$ 조절 T 세포의 수가 동시에 크게 증가하여, 항암 T 세포의 기능을 억제하는 기전이 경부 임파절에서 동시에 일어남을 확인할 수 있었다.

주요어 : 구강 편평세포암종, 악성암화, 전암병소, 조절 T 임파구, 세포독성 T 임파구, 종양 미세환경

학 번 : 2021-29761